

Synthesis, structural and spectroscopic characterization of mono- and binuclear copper(I) complexes with substituted diimine and phosphine ligands

Wen-Fu Fu^{a,b,*}, Xin Gan^a, Jian Jiao^a, Yong Chen^b, Mei Yuan^b, Shao-Ming Chi^a,
Ming-Ming Yu^b, Shao-Xiang Xiong^c

^a College of Chemistry and Chemical Engineering, Yunnan Normal University, Kunming 650092, PR China

^b Technical Institute of Physics and Chemistry, Chinese Academy of Sciences, Peking 100080, PR China

^c Beijing Mass spectrometry Center, Center for Molecular Science, Institute of Chemistry, Chinese Academy of Sciences, Beijing 100080, PR China

Received 15 November 2006; received in revised form 9 February 2007; accepted 9 February 2007

Available online 20 February 2007

Abstract

The reaction of $[\text{Cu}(\text{CH}_3\text{CN})_4]\text{BF}_4$, 6-(4-methoxy)phenyl-2,2'-bipyridine (designated as MeO-CNN), and/or tricyclohexylphosphine (PCy_3) and diimine ligands derived from 4,4'-bipyridine gave four mono- and binuclear copper(I) complexes, $[\text{Cu}(\text{MeO-CNN})_2]\text{BF}_4$ (**1**), $[\text{Cu}_2(\text{MeO-CNN})_2(\text{PCy}_3)_2(4,4'\text{-bipy})](\text{BF}_4)_2 \cdot 1.5\text{CH}_2\text{Cl}_2$ (**2**) (bipy = bipyridine), $[\text{Cu}_2(\text{MeO-CNN})_2(\text{PCy}_3)_2(\text{bpete})](\text{BF}_4)_2 \cdot 4\text{CH}_2\text{Cl}_2$ (**3**) (bpete = *trans*-1,2-bis(4-pyridyl)ethene) and $[\text{Cu}_2(\text{MeO-CNN})_2(\text{PCy}_3)_2(4,4'\text{-azpy})](\text{BF}_4)_2 \cdot 1.5\text{CH}_2\text{Cl}_2$ (**4**) (azpy = azobispyridine). Crystallographic studies of complexes **1–4** show that each copper(I) center adopts a pseudo-tetrahedral coordination geometry. Complexes **2–4** consists of $-\text{Cu}(\text{MeO-CNN})(\text{PCy}_3)$ units which are linked through 4,4'-bipy, bpete and 4,4'-azpy, respectively. The UV–Vis spectra of these four complexes all exhibit intense high-energy absorptions at $\lambda_{\text{max}} < 340$ nm and broad visible bands in a range of 430–550 nm, ascribed to intraligand ($\text{IL } \pi \rightarrow \pi^*$) transitions and metal-to-ligand charge-transfer (MLCT) transitions, respectively. The density functional theory calculation was used to interpret the absorption spectrum of **1**, which further supports the assignment of MLCT character. The binuclear complexes **2** and **3** both display red solid-state emissions centred at 620 and 660 nm from metal-to-ligand charge-transfer excited state, respectively. Interestingly, the electron paramagnetic resonance (EPR) spectral measurements confirm copper(I) complexes oxidized to corresponding copper(II)–halide product upon excitation at 355 nm in dichloromethane solution.

© 2007 Elsevier B.V. All rights reserved.

Keywords: Copper(I) complexes; Aromatic diimine; Phosphine; Photophysical properties; Crystal structures

1. Introduction

Copper(I) complexes containing diimine and/or phosphine ligands have been extensively studied for their photophysical properties, photoinduced electron-transfer reactions and excited-state substrate-binding reactions [1–5]. These complexes display a variety of long-lived emissive electronic excited states. Depending on the nature of polypyridine ligand, metal-centered (MC or d–d), metal-to-

ligand charge-transfer (MLCT or d– π^*), or intraligand excited state (IL or π – π^*) can be the lowest energy electronic excited state [6–10]. A subtle change in the electronic property of polypyridine ligand has been reported to alter the nature of the lowest excited state in these complexes [11,12]. In the literatures, applications of copper(I) complexes containing diimine or phosphine ligands in luminescent sensing and light-induced generation of hydrogen from water have been investigated [13,14]. A remarkable amount of work has been devoted to characterization of the excited-state redox properties and the kinetic analysis of excited-state electron-transfer reactions of these kinds of complexes [15–17]

* Corresponding author. Tel.: +86 10 8254 3519; fax: +86 10 6255 4670.
E-mail address: wf_fu@yahoo.com.cn (W.-F. Fu).

Complexes with 1,10-phenanthroline ligand that possesses alkyl or aryl substituent at the 2- and 9-positions display low-energy MLCT transition and weak photoluminescence in the visible region [18,19]. In general, bulky 2- and 9-substituents of 1,10-phenanthroline ligand can lead to an increase in emission quantum yield [20]. Although the photophysical properties of copper(I) phenanthroline complexes have been extensively studied, related studies on copper(I) complexes containing bulky phosphine, such as tricyclohexylphosphine (PCy₃) substituted 2,2'-bipyridine and 4,4'-bipyridine derivatives bridging ligands are elusive [21]. Herein, we successfully designed and obtained four mono- and binuclear copper(I) complexes in the presence of 6-(4-methoxy)phenyl-2,2'-bipyridine (MeO-CNN) [22] and/or 4,4'-bipyridine derivatives and phosphine ligands, [Cu(MeO-CNN)₂](BF₄)₂ (1), [Cu₂(MeO-CNN)₂(PCy₃)₂(4,4'-bipy)](BF₄)₂ · 1.5CH₂Cl₂ (2) (bipy = bipyridine), [Cu₂(MeO-CNN)₂(PCy₃)₂(bpete)](BF₄)₂ · 4CH₂Cl₂ (3) (bpete = *trans*-1,2-bis(4-pyridyl)ethene) and [Cu₂(MeO-CNN)₂(PCy₃)₂(4,4'-azpy)](BF₄)₂ · 1.5CH₂Cl₂ (4) (azpy = azobispyridine). Their structures, thermal stability and spectroscopic properties were also investigated.

2. Experimental

2.1. Materials and reagents

N-(Pyridincarbonylmethyl)pyridinium iodide and [Cu(CH₃CN)₄](BF₄) were prepared according to the published literature [23]. 2-Acetyl pyridine (Acros, 98%), tricyclohexylphosphine (Acros, 98%), 1,2-bis(4-pyridyl)ethene (Aldrich, 97%), and 4,4'-bipyridine (Acros, 98%) were commercially available and used as purchased without further purification. All of the solvents obtained from commercial sources were purified and distilled by standard procedures prior to use.

2.2. Synthesis

2.2.1. Synthesis of the *p*-methoxyacetophenone

To a mixture of anisole (10.8 g, 0.1 mol) and acetic anhydride (11.3 g, 0.11 mol), iodine (0.50 g, 0.002 mol) was added. The reaction mixture was heated to reflux for 4 h. The dark brown solution was poured into water (50 mL) and extracted with diethyl ether (3 × 50 mL). The diethyl ether solution was washed successively with dilute sodium carbonate, water and dried over sodium sulfate. After removal of the solvent and purification of the residue under vacuum, *p*-methoxyacetophenone was obtained. Yield: 10 g (67%), m.p. 36–37 °C, which is comparable to the value reported (38 °C) [24].

2.2.2. Synthesis of the β-(dimethylamino)-4'-methoxypropionophenone hydrochloride

To a solution of *p*-methoxyacetophenone (7.5 g, 0.05 mol) and dimethylamine hydrochloride (5.27 g, 0.065 mol) in ethanol (20 mL), paraformaldehyde (2.0 g,

0.22 mol) was added, and followed by 1 mL of concentrated hydrochloric acid (HCl, 37%) [25]. The mixture was refluxed for 2 h. When the solution was warm, it was diluted by addition of acetone (100 mL), allowed to cool slowly to room temperature, and kept overnight in the refrigerator. A white product was collected and washed with acetone. After dryness for 3 h at 40–50 °C, the product was obtained (7.6 g, 62%). *Anal.* Calc. for C₁₂H₁₈ClNO₂: C, 59.13; H, 7.44; N, 5.75. Found: C, 59.36; H, 7.11; N, 5.56%.

2.2.3. Synthesis of the 6-(4-methoxyphenyl)-2,2'-bipyridine

To a mixture of 1-(2-pyridylcarbonylmethyl)pyridinium iodide (6.50 g, 0.02 mol) and ammonium acetate (10 g) in ethanol (40 mL), β-(dimethylamino)-4'-methoxypropionophenone hydrochloride (4.87 g, 0.02 mol) was added [26]. The mixture was heated to reflux for 3 h. The dark green solution was cooled and the green crude product was filtered, washed with water and cold ethanol. The product was purified by chromatography on silica gel column with petroleum spirit–ethyl acetate (5:1) as the eluent. Yield: 1.5 g (29%). FT-IR (KBr disc): ν 2900 (w), 1607 (m), 1582 (s), 1559 (m), 1514 (s), 1453 (s), 1421 (s), 1247 (s), 1022 (m) cm⁻¹. ¹H NMR (400 MHz, CDCl₃): δ 4.36 (s, 3H), 7.55 (d, *J* = 8 Hz, 2H), 7.66 (m, 1H), 7.88 (d, *J* = 8 Hz, 1H), 8.01 (m, 1H), 8.14 (d, *J* = 8 Hz, 1H), 8.21 (m, 2H), 8.63 (d, *J* = 8 Hz, 1H), 8.78 (d, *J* = 8 Hz, 1H), 8.95 (d, *J* = 5 Hz, 1H). ESI-MS: *m/z* 262.31 [M⁺]. *Anal.* Calc. for C₁₇H₁₄N₂O: C, 77.84; H, 5.38; N, 10.68. Found: C, 77.67; H, 5.16; N, 10.38%.

2.2.4. Synthesis of the 4,4'-azopyridine (4,4'-azpy)

4,4'-Azopyridine(4,4'-azpy) was prepared through the oxidative coupling of 4-aminopyridine by hypochlorite according to published procedures [27]. Yield: 80%. *Anal.* Calc. for C₁₀H₈N₄: C, 65.21; H, 4.38; N, 30.42. Found: C, 65.40; H, 4.53; N, 30.65%.

2.2.5. Synthesis of [Cu(MeO-CNN)₂](BF₄)

A mixture of [Cu(CH₃CN)₄](BF₄) (0.157 g, 0.5 mmol) and L (0.262 g, 1 mmol) in dichloromethane (30 mL) was stirred under nitrogen atmosphere at room temperature for 2 h. Then the solvents were removed and the solid residue was afforded. Recrystallization by slow diffusion of diethyl ether into a dichloromethane solution yielded dark crystals suitable for X-ray diffraction. Yield: 0.277 g (82%). ¹H NMR (400 MHz, DMSO-*d*₆): 3.61 (s, 6H, -OMe), 6.32 (s, 4H), 7.31 (s, 4H), 7.66 (m, 4H), 8.02 (t, *J* = 7.8, 2H), 8.20 (t, *J* = 7.8, 2H), 8.25 (d, *J* = 7.8, 2H), 8.46 (d, *J* = 7.9, 2H), 8.60 (d, *J* = 3.1, 2H). *Anal.* Calc. for C₃₄H₂₈BCuF₄N₄O₂ (powders): C, 60.50; H, 4.18; N, 8.30. Found: C, 60.83; H, 4.02; N, 8.19% [22].

2.2.6. Synthesis of [Cu₂(MeO-CNN)₂(PCy₃)₂(4,4'-bipy)](BF₄)₂ · 1.5CH₂Cl₂

Under nitrogen atmosphere, a mixture of L (0.262 g, 1 mmol) and [Cu(CH₃CN)₄](BF₄) (0.315 g, 1 mmol) in

dichloromethane (30 mL) was stirred at room temperature for 2 h. Then tricyclohexylphosphine (0.280 g, 1 mmol) in dichloromethane (5 mL) was dropped to the solution with stirring followed by the addition of 4,4'-bipy (0.078 g, 0.5 mmol). After stirring the resultant solution for another 12 h, the solvents were removed and the solid residue was obtained. Recrystallization by slow diffusion of diethyl ether into a dichloromethane solution yielded yellow crystals suitable for X-ray diffraction. Yield: 0.602 g (78%). ^1H NMR (400 MHz, DMSO- d_6): 1.02–1.14 (m, 32H, Cy), 1.47 (s, 16H, Cy), 1.60 (s, 18H, Cy), 3.83 (s, 6H, –OMe), 7.08 (s, 4H), 7.58 (s, 4H), 7.78 (s, 2H), 7.92 (s, 4H), 8.02 (s, 2H), 8.07 (s, 4H), 8.21 (t, $J = 7.6$, 4H), 8.46 (s, 2H), 8.57 (d, $J = 7.8$, 2H), 8.75 (s, 2H). ^{31}P NMR (DMSO- d_6): 17.46. *Anal.* Calc. for $\text{C}_{80}\text{H}_{102}\text{B}_2\text{Cu}_2\text{F}_8\text{N}_6\text{O}_2\text{P}_2$ (powders): C, 62.30; H, 6.67; N, 5.45. Found: C, 62.55; H, 6.73; N, 5.47%.

2.2.7. Synthesis of $[\text{Cu}_2(\text{MeO-CNN})_2(\text{PCy}_3)_2(\text{bpete})](\text{BF}_4)_2 \cdot 4\text{CH}_2\text{Cl}_2$

Complex **3** was prepared in a similar way to complex **2** except that bpete was used in place of 4,4'-bipy. The yellow crystals were obtained suitable for X-ray diffraction. Yield: 0.565 g (72%). ^1H NMR (400 MHz, DMSO- d_6): 1.06–1.26 (m, 32H, Cy), 1.59 (s, 34H, Cy), 3.79 (s, 6H, –OMe), 7.02 (s, 4H), 7.52 (d, $J = 3.5$, 8H), 7.76 (t, 4H), 7.97 (s, 2H), 8.20 (t, 4H), 8.44–8.71 (m, 10H). ^{31}P NMR (DMSO- d_6): 18.11. *Anal.* Calc. for $\text{C}_{82}\text{H}_{104}\text{B}_2\text{Cu}_2\text{F}_8\text{N}_6\text{O}_2\text{P}_2$ (powders): C, 62.80; H, 6.68; N, 5.36. Found: C, 62.57; H, 6.77; N, 5.39%.

2.2.8. Synthesis of $[\text{Cu}_2(\text{MeO-CNN})_2(\text{PCy}_3)_2(4,4'\text{-azpy})](\text{BF}_4)_2 \cdot 1.5\text{CH}_2\text{Cl}_2$

The preparation of complex **4** was also similar to that of complex **2** except that 4,4'-bipy was replaced by 4,4'-azpy. The dark red crystals were obtained suitable for X-ray diffraction. Yield: 0.597 g (76%). ^1H NMR (400 MHz, DMSO- d_6): 1.01–1.09 (m, 32H, Cy), 1.45 (s, 16H, Cy), 1.57 (s, 18H, Cy), 3.84 (s, 6H, –OMe), 7.10 (d, $J = 7.0$, 4H), 7.61 (s, 4H), 7.80 (s, 2H), 7.95 (s, 4H), 8.02 (d, $J = 6.4$, 2H), 8.10 (d, $J = 7.2$, 4H), 8.22 (t, $J = 7.1$, 4H), 8.48 (d, $J = 6.7$, 2H), 8.57 (d, $J = 7.5$, 2H), 8.77 (s, 2H). ^{31}P NMR (DMSO- d_6): 17.45. *Anal.* Calc. for $\text{C}_{80}\text{H}_{102}\text{B}_2\text{Cu}_2\text{F}_8\text{N}_8\text{O}_2\text{P}_2$ (powders): C, 61.19; H, 6.55; N, 7.14. Found: C, 61.37; H, 6.67; N, 7.40%.

2.3. Photophysical measurements

UV–Vis absorption spectra were recorded using Hitachi U-3010 spectrophotometer. Emission and excitation spectra were performed with Hitachi F-4500 fluorescence spectrometer. ^1H NMR spectra were obtained on a Bruker Avance DPX-400 MHz Resonance Spectrometer. The EPR spectra were recorded on a Bruker Electron Spin Resonance Meter ER046 with an X band Microwave Bridge.

2.4. X-ray structure determination

Crystals of complexes **1–4** suitable for X-ray structure analysis were grown from dichloromethane solution by

Table 1
Summary of X-ray crystallographic data for complexes **1–4**

Compound	1	2	3	4
Formula	$\text{C}_{34}\text{H}_{28}\text{BCuF}_4\text{N}_4\text{O}_2$	$\text{C}_{81.5}\text{H}_{105}\text{B}_2\text{Cl}_3\text{Cu}_2\text{F}_8\text{N}_6\text{O}_2\text{P}_2$	$\text{C}_{86}\text{H}_{112}\text{B}_2\text{Cl}_8\text{Cu}_2\text{F}_8\text{N}_6\text{O}_2\text{P}_2$	$\text{C}_{81.5}\text{H}_{105}\text{B}_2\text{Cl}_3\text{Cu}_2\text{F}_8\text{N}_8\text{O}_2\text{P}_2$
Formula weight	674.95	1669.70	1908.06	1697.72
Space group	$P2_1/n$	$P\bar{1}$	$P\bar{1}$	$P2_1/n$
Crystal system	monoclinic	triclinic	triclinic	monoclinic
a (Å)	15.4093(7)	15.050(5)	13.884(5)	9.650(10)
b (Å)	11.5488(4)	17.712(7)	14.205(5)	26.49(3)
c (Å)	17.5000(6)	18.366(9)	14.766(5)	17.001(19)
α (°)	90	102.052(9)	116.176(5)	90
β (°)	96.514(2)	97.512(10)	98.706(6)	93.01(2)
γ (°)	90	94.972(9)	108.948(5)	90
V (Å ³)	3094.2(2)	4714(3)	2318.2(14)	4341(8)
Z	4	2	1	2
T (K)	293(2)	293(2)	293(2)	293(2)
ρ_{calc} (g cm ^{−3})	1.449	1.176	1.367	1.299
θ Range (°)	2.12–27.48	1.92–25.00	1.67–26.38	2.25–25.00
μ (mm ^{−1})	0.768	0.629	0.788	0.685
Observed data	7061	16368	9332	7567
Number of parameters	415	1094	617	571
R_1^a	0.0467	0.0786	0.0571	0.0806
wR_2^a	0.0965	0.1904	0.1345	0.1811
Maximum and minimum peaks (e Å ^{−3})	0.748 and −0.306	0.800 and −0.301	0.707 and −0.422	0.537 and −0.416

^a $I > 2\sigma(I)$, $R_1 = \sum |F_o| - |F_c| / \sum |F_o|$, $wR_2 = \{ \sum [w(F_o^2 - F_c^2)^2] / \sum [w(F_o^2)^2] \}^{1/2}$.

Table 2
Selected bond lengths (Å) and angles (°) for **1–4**

Complex 1			
Cu–N(1)	2.042(3)	Cu–N(2)	2.040(3)
Cu–N(3)	2.082(3)	Cu–N(4)	2.015(3)
N(1)–C(7)	1.355(4)	N(2)–C(12)	1.331(4)
N(3)–C(23)	1.355(4)	N(4)–C(28)	1.354(4)
N(1)–Cu–N(2)	81.06(12)	N(1)–Cu–N(3)	115.74(10)
N(3)–Cu–N(4)	81.57(12)	N(4)–Cu–N(2)	107.93(12)
N(1)–Cu–N(4)	144.60(11)	N(2)–Cu–N(3)	136.89(11)
N(1)–C(7)–C(4)	118.3(3)	N(1)–C(11)–C(12)	115.6(3)
Complex 2			
Cu(1)–N(1)	2.125(5)	Cu(1)–N(2)	2.091(5)
Cu(1)–N(3)	2.054(5)	Cu(1)–P(1)	2.2058(17)
C(5)–C(6)	1.455(9)	C(10)–C(11)	1.474(9)
C(20)–C(20)*	1.467(10)		
N(1)–Cu(1)–N(3)	100.8(2)	N(1)–Cu(1)–N(2)	78.5(2)
N(1)–Cu(1)–P(1)	111.72(15)	N(2)–Cu(1)–P(1)	119.61(14)
N(3)–Cu(1)–P(1)	119.72(14)	N(2)–Cu(1)–N(3)	115.67(19)
C(23)–P(1)–Cu(1)	116.7(2)	N(1)–C(5)–C(6)	116.4(6)
C(4)–C(5)–C(6)	123.0(7)	C(9)–C(10)–C(11)	118.8(7)
N(2)–C(10)–C(11)	119.0(6)	C(19)–C(20)–C(20)*	122.4(6)
Complex 3			
Cu(1)–N(1)	2.121(4)	Cu(1)–N(2)	2.163(4)
Cu(1)–N(3)	2.066(3)	Cu(1)–P(1)	2.2224(12)
C(5)–C(6)	1.445(7)	C(10)–C(11)	1.455(7)
C(20)–C(23)*	1.461(5)	C(23)–C(23)*	1.301(8)
N(1)–Cu(1)–N(3)	100.68(13)	N(1)–Cu(1)–N(2)	78.16(16)
N(1)–Cu(1)–P(1)	118.89(10)	N(2)–Cu(1)–P(1)	112.50(9)
N(3)–Cu(1)–P(1)	122.58(10)	N(2)–Cu(1)–N(3)	115.21(13)
C(24)–P(1)–Cu(1)	111.43(14)	N(1)–C(5)–C(6)	117.6(4)
C(4)–C(5)–C(6)	123.3(6)	C(9)–C(10)–C(11)	118.8(5)
N(2)–C(10)–C(11)	120.5(4)	C(20)–C(23)–C(23)*	125.8(5)
Complex 4			
Cu(1)–N(1)	2.110(3)	Cu(1)–N(2)	2.120(3)
Cu(1)–N(3)	2.071(3)	Cu(1)–P(1)	2.220(2)
C(5)–C(6)	1.450(6)	C(10)–C(11)	1.471(6)
N(1)–C(5)	1.356(5)	C(20)–N(4)	1.439(4)
N(4)–N(4)*	1.242(5)		
N(1)–Cu(1)–N(3)	99.27(13)	N(1)–Cu(1)–N(2)	77.53(13)
N(1)–Cu(1)–P(1)	112.54(9)	N(2)–Cu(1)–P(1)	119.20(9)
N(3)–Cu(1)–P(1)	123.16(9)	N(2)–Cu(1)–N(3)	112.74(13)
C(23)–P(1)–Cu(1)	113.22(12)	N(1)–C(5)–C(6)	116.2(3)
C(4)–C(5)–C(6)	124.8(4)	C(9)–C(10)–C(11)	121.4(4)
N(2)–C(10)–C(11)	117.9(3)	C(19)–C(20)–N(4)	116.4(3)
C(20)–N(4)–N(4)*	112.4(4)		

slow diffusion of diethyl ether over the period of several days. The diffraction data were collected at room temperature with graphite-monochromatized Mo K α radiation ($\lambda = 0.71073$ Å) on a Rigaku R-Axis RAPID IP X-ray diffractometer. An absorption correction was applied by correction of symmetry-equivalent reflections using the ABCOR program. The structure was solved by direct methods using the SHELXS-97 program and refined by full-matrix least-squares on F^2 using the SHELXL-97 software [28]. The hydrogen atoms were added using ideal geometries with a fixed C–H bond distance. The relevant crystallographic data as well as selected bond distances and angles for complexes **1–4** were listed in Tables 1 and 2, respectively.

2.5. Computational methods

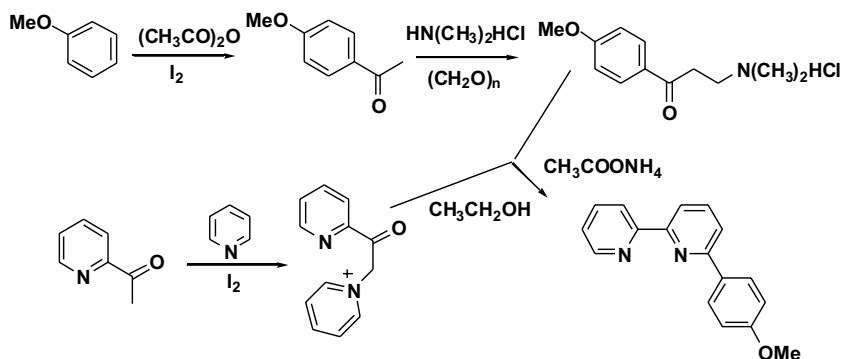
The density functional theory calculation of complex **1** was carried out using the GAUSSIAN-03 suite of programs [29], at the B3LYP level. The basis set used for C, N, O and H atoms was 6-31G while effective core potentials with a LanL2DZ basis set were employed for transition metals. The contour plots of MOs were obtained with the GAUSSIAN-03 view program.

3. Results and discussion

3.1. Syntheses of ligand *L* and complexes

The ligand 6-(4-methoxy)phenyl-2,2'-bipyridine was firstly synthesized according to a standard Kröhnke procedure outlined in Scheme 1, in which the central pyridyl ring is generated by the condensation of a 1,5-dicarbonyl intermediate (obtained from the Michael reaction of *N*-(pyridin-carbonylmethyl)pyridinium iodide and (β -dimethyl)aminopropio(4-methoxy)phenone) with a large excess of ammonium acetate [26].

The reaction of a dichloromethane solution of $[\text{Cu}(\text{CH}_3\text{CN})_4]\text{BF}_4$ and MeO-CNN ligand in a 1:2 molar ratio under a nitrogen atmosphere afforded mononuclear complex **1** as a modera solid upon precipitation by diethyl ether. By introducing tricyclohexylphosphine (PCy_3) and a series of diimine ligands (4,4'-bipy, bpete, and 4,4'-azpy) in



Scheme 1.

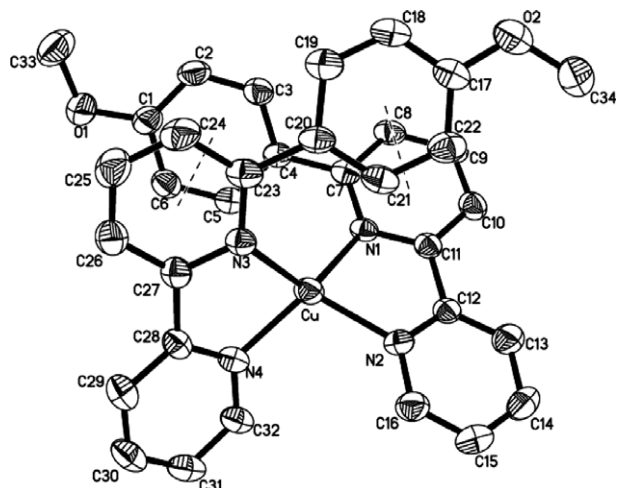


Fig. 1. Perspective drawing of $[\text{Cu}(\text{MeO-CNN})_2]\text{BF}_4$ (**1**). The thermal ellipsoids are drawn at 30% probability.

a similar reaction manner to $\text{Cu}(\text{MeO-CNN})(\text{CH}_3\text{CN})_2\text{-BF}_4$, other three dinuclear copper(I) complexes **2–4** were obtained with subtle structure changes.

3.2. Crystal structures of complexes **1–4**

Single-crystal X-ray analysis shows that the Cu(I) center of mononuclear complex **1** is in a pseudo-tetrahedral geometry, and the coordinated 2,2'-bipyridine fragments of MeO-CNN ligands are not coplanar with the dihedral angles of 9.3° and 22.7° . The MeO-substituted phenyl rings are twisted with respect to their bonded pyridine fragments with torsion angles of 38.1° and 24.0° for two MeO-CNN ligands, respectively. An ORTEP view with atom numbering for the cation is illustrated in Fig. 1. The Cu–N bond lengths vary from 2.015 Å to 2.082 Å and the N–Cu–N angles range from 81.06° to 144.6° (Tables 1 and 2). Interestingly, interligand π – π stacking interactions in molecule are observed between the phenyl ring and the pyridyl ring, resulting in a interplanar separation of 3.5 Å. In the space packing of **1** (Fig. S1), there exist plenty of weak hydrogen bonds between the O(1) atom of the methoxyl substituent or F(1) atoms of the BF_4^- anion and the carbon atoms of the MeO-CNN ligands, with $\text{C}\cdots\text{O}$ and $\text{C}\cdots\text{F}$ distances about 3.4 Å. The relevant hydrogen-bonding distances and angles are listed in Table (S).

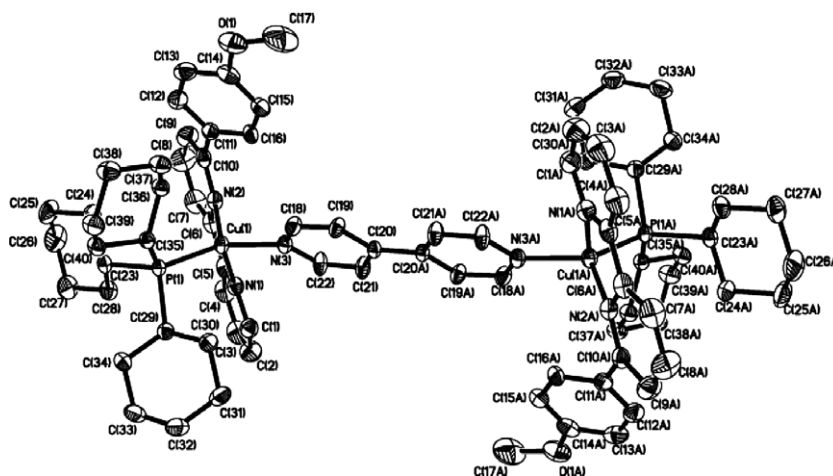


Fig. 2. Perspective drawing of $[\text{Cu}_2(\text{MeO-CNN})_2(\text{PCy}_3)_2(4,4'\text{-bipy})](\text{BF}_4)_2 \cdot 1.5\text{CH}_2\text{Cl}_2$ (**2**). The thermal ellipsoids are drawn at 30% probability.

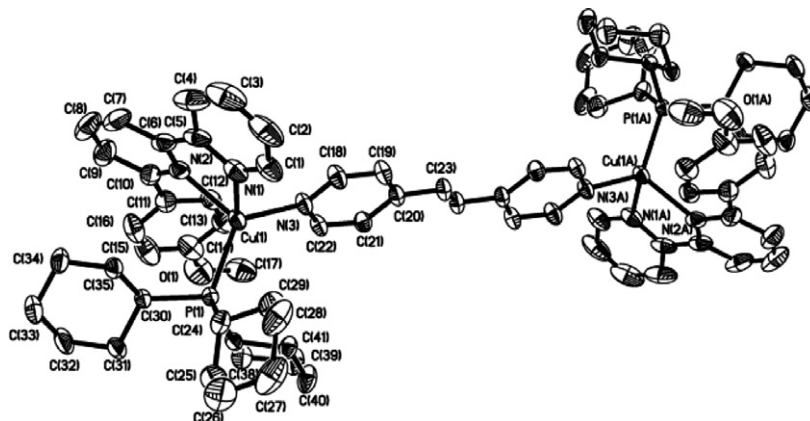


Fig. 3. Perspective drawing of $[\text{Cu}_2(\text{MeO-CNN})_2(\text{PCy}_3)_2(\text{bpete})](\text{BF}_4)_2 \cdot 4\text{CH}_2\text{Cl}_2$ (**3**). The thermal ellipsoids are drawn at 30% probability.

The molecular structures of complexes **2–4** with different bridging ligands are analogous to each other (Figs. 2–4 and Tables 1 and 2). Each copper in all three complexes is ligated to two nitrogen atoms of MeO-CNN, one phosphorus atom of PCy₃, forming PCuN₂⁺ unit. The two PCuN₂⁺ fragments are further linked together into a binuclear form by 4,4'-bipy, bpete and 4,4'-azpy for complexes **2–4**, respectively, showing a center of symmetry.

As expected, the phenyl ring is substantially twisted away from the plane of the bipyridine segment of MeO-CNN. The coordinated bipyridine fragments of MeO-CNN in complexes **2–4** are not coplanar having the dihedral angles of 5.8° for **2**, 16.7° for **3**, and 3.1° for **4**, which are compared with the torsion angles of 44.8° for **2**, 38.6° for **3**, and 46.6° for **4** between the terminal aromatic ring and its adjacent pyridyl ring. However, the two pyridyl rings of the kind of bridging bipy ligands (4,4'-bipy, bpete, and 4,4'-azpy) in these three complexes are almost coplanar. In complex **3**, intermolecular C(8)⋯C(21) contact of 3.387 Å at pyridyl rings of MeO-CNN and bridging bpete ligands in different molecules is indicative of two pyridyl rings of MeO-CNN ligand having larger torsion. The copper center lies closer to the nitrogen atom of the bridging ligand (average bond distance at 2.064 (4) Å) than it does to those nitrogen atoms from the chelating MeO-CNN ligand (average bond distance at 2.122 (4) Å). The intramolecular Cu(I)⋯Cu(I) separations among the complexes **2–4** are 11.194 Å, 12.436 Å and 13.130 Å, respectively. Furthermore, similar weak hydrogen-bonding interactions to complex **1** are also found between the fluorine atoms of the BF₄[−] anion and the carbon atoms from the MeO-CNN ligands, but the relevant C⋯F distances are relatively closer than that in complex **1** (the details are listed in Table (S) and Figs. S2–S4).

3.3. Thermogravimetric analysis

The powder samples of complexes **1–4** without solvents were analysed using a TGA apparatus under 20 mL min^{−1} flowing nitrogen (Figs. S5–S7). The temperature was ramped at a rate of 20 °C min^{−1} from 40 to 500 °C. The

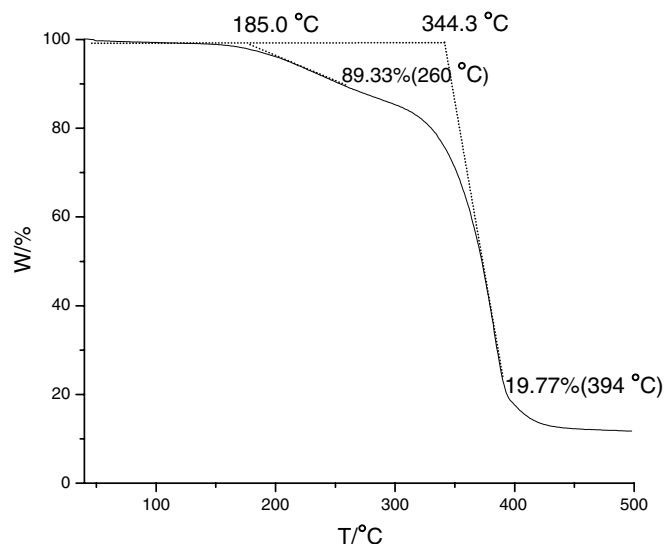


Fig. 5. TG curve of complex **2** in N₂.

intermediate stages of decomposition were readily assigned for these complexes. For **1** the results of TGA showed an initial mass loss corresponding to the loss of MeO-CNN ligands. This loss process at about 360–500 °C leads to the residue in accordance to a stoichiometry of CuBF₄. Complexes **2–4** are stable to air and moisture, but the two-step weight loss for the complexes were observed, in which the primary formation of intermediate (MeO-CNN)Cu(PCy₃)BF₄, commencing at 185–260 °C, is followed by the subsequent formation of CuBF₄ at about 344–394 °C (Fig. 5). According to the above results, complex **1** seems to have a higher thermal stability than complexes **2–4**, which also agrees well with their structural characters that the Cu–N distances of the copper center coordinated to two chelating MeO-CNN ligands in **1** are significantly shorter than those of complexes **2–4** containing bridging 4,4'-bipyridine derivatives.

3.4. Absorption and emission spectra

The electronic absorption spectra for complexes **1–4** all include a series of high-energy intraligand transition and

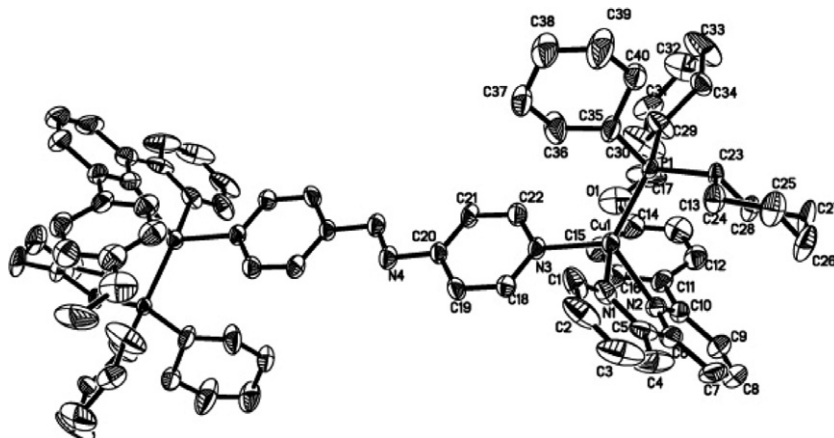


Fig. 4. Perspective drawing of [Cu₂(MeO-CNN)₂(PCy₃)₂(4,4'-azpy)](BF₄)₂ · 1.5CH₂Cl₂ (**4**). The thermal ellipsoids are drawn at 30% probability.

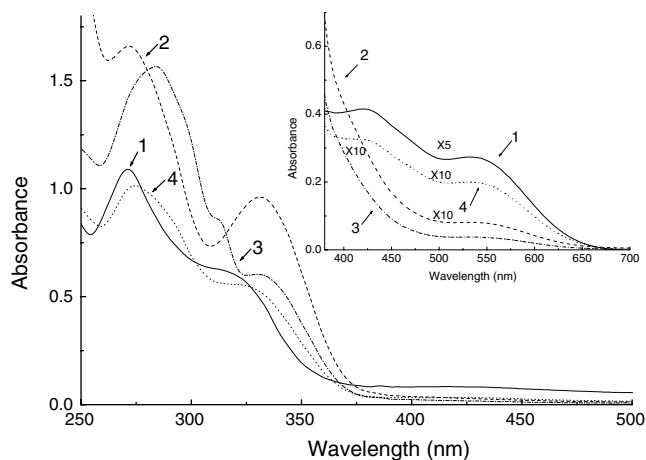


Fig. 6. The electronic absorption spectra of $[\text{Cu}(\text{MeO-CNN})_2]\text{BF}_4$ (1) (solid line), $[\text{Cu}_2(\text{MeO-CNN})_2(\text{PCy}_3)_2(4,4'\text{-bipy})](\text{BF}_4)_2 \cdot 1.5\text{CH}_2\text{Cl}_2$ (2) (dash line), $[\text{Cu}_2(\text{MeO-CNN})_2(\text{PCy}_3)_2(\text{bpete})](\text{BF}_4)_2 \cdot 4\text{CH}_2\text{Cl}_2$ (3) (dash dot line), and $[\text{Cu}_2(\text{MeO-CNN})_2(\text{PCy}_3)_2(4,4'\text{-azpy})](\text{BF}_4)_2 \cdot 1.5\text{CH}_2\text{Cl}_2$ (4) (dot line) in dichloromethane solution at room temperature. Inset: long wavelength region of the electronic absorption spectra of 1–4.

low-energy charge-transfer absorption (Fig. 6). Each of these complexes shows an intense and broad band at λ_{max} 425–550 nm, which tails beyond 650 nm in dichloromethane solution at room temperature. The intense absorptions at $\lambda_{\text{max}} < 340$ nm are assigned to intraligand (IL $\pi \rightarrow \pi^*$) transitions, which can be compared with the absorptions of the free ligands. The low-energy absorption bands at 425 and 550 nm for the complexes are characteristic for MLCT transition [1,30]. The density functional theory calculation of complex 1 was performed to interpret the electronic character of absorption spectra. The relevant highest-occupied molecular orbital (HOMO) and lowest-

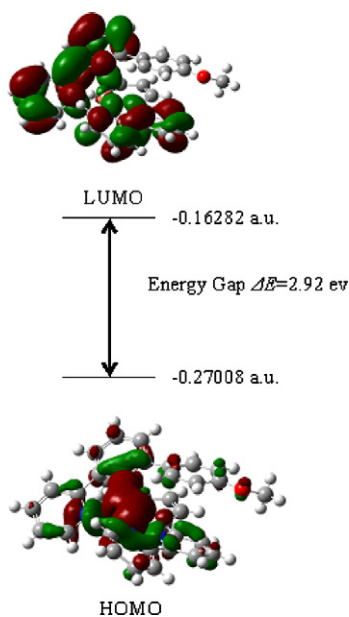


Fig. 7. Contour plots and orbital energies of the HOMO and LUMO for $[\text{Cu}(\text{MeO-CNN})_2]\text{BF}_4$.

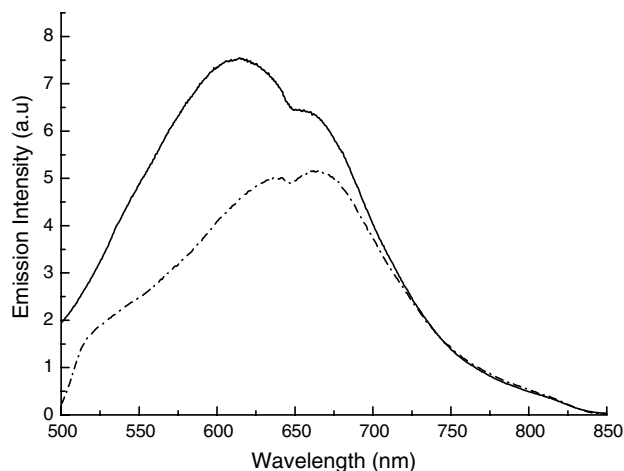


Fig. 8. Room-temperature solid-state emission spectra of $[\text{Cu}_2(\text{MeO-CNN})_2(\text{PCy}_3)_2(4,4'\text{-bipy})](\text{BF}_4)_2 \cdot 1.5\text{CH}_2\text{Cl}_2$ (2) (solid line) $[\text{Cu}_2(\text{MeO-CNN})_2(\text{PCy}_3)_2(\text{bpete})](\text{BF}_4)_2 \cdot 4\text{CH}_2\text{Cl}_2$ (3) (dash dot line) upon excitation at 420 nm.

unoccupied molecular orbital (LUMO) together with the orbital energies, are showed in the contour plots in Fig. 7. The character of the HOMO is dominated by the d orbital of Cu, whereas the LUMO is mainly localized on the pyridyl rings and displays π^* character. The calculations HOMO–LUMO gap 2.92 eV (425 nm) is essentially consistent with the experimental results described as MLCT character.

Compared with complex 2, complex 3 represents typical spectral changes (bpete) with a shoulder peak at 312 nm, while the characteristic spectrum (4,4'-azpy) of complex 4 is not observed due to the absorption overlapping. Upon excitation at 420 nm, complexes 2 and 3 exhibit weak photoluminescence with λ_{max} at 620 nm ($\tau = 0.17 \mu\text{s}$) and 660 nm ($\tau = 0.23 \mu\text{s}$) in the solid state at room temperature, respectively (Fig. 8). The emission spectra of complexes 2 and 3 are extremely similar, whereas there is no significant emission observed in the same measuring conditions for complexes 1 and 4. With reference to the previous work, the red emissions are assigned to the MLCT triple excited state [1]. All complexes are non-emissive in dichloromethane or acetonitrile solutions

3.5. Photoinduced electron-transfer

We observed photoinduced electron transfer reactions of the Cu(I) complexes in dichloromethane solution at ambient temperature, whereas no noticeable reaction was found in pure CH_3CN or $(\text{CH}_3)_2\text{SO}$ solution. EPR spectra for complexes 1–4 were recorded upon an excitation of 355 nm at 298 K in degassed dichloromethane solution. As shown in Fig. 9, upon irradiation, the characteristic intensity of the EPR signals at 3200–3400 G were clearly observed in complexes 1 and 2 with methylviologen (MV^{2+}), indicating the formation of copper(II) species in dichloromethane solution [31,32]. Similar EPR results have been also found for complexes 3–4 in dichloromethane

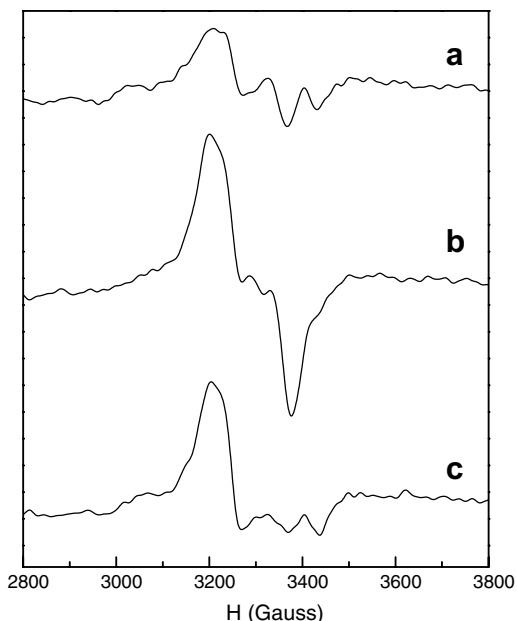


Fig. 9. EPR spectra of $[\text{Cu}(\text{MeOCNN})_2]\text{BF}_4$ with methylviologen (a), $[\text{Cu}_2(\text{MeOCNN})_2(\text{PCy}_3)_2(\text{bipy})](\text{BF}_4)_2$ with methylviologen (b) and $[\text{Cu}_2(\text{MeOCNN})_2(\text{PCy}_3)_2(\text{bipy})](\text{BF}_4)_2$ (c) upon excitation at 355 nm at 298 K in dichloromethane solution.

solution and the absence of MV^{2+} . Formation of Cu(II) species has previously been found in the reaction of copper(I) complexes with benzyl halides in the presence of CH_2Cl_2 or CHCl_3 [33–35]. Based on the EPR studies, we deduced the process of the photoinduced electron transfer reaction as: upon irradiation with light at 355 nm, the Cu(I) complexes underwent oxidative addition with Cu–Cl bond formation. With excitation of the copper complexes into the MLCT transition, the electron density is shifted from Cu(I) to the conjugated aromatic diimines, which enables a possible attack of the vacant on Cu(I) center and electrophilic metal site for reaction with CH_2Cl_2 to give corresponding copper(II)–halide complex [36].

4. Conclusions

By introducing a chelating ligand 6-(4-methoxy)phenyl-2,2'-bipyridine (MeO-CNN), one mononuclear copper(I) complex $[\text{Cu}(\text{MeO-CNN})_2]\text{BF}_4$ (**1**), and three dinuclear complexes $[\text{Cu}_2(\mu\text{-diimine})(\text{MeO-CNN})_2(\text{PCy}_3)_2](\text{BF}_4)_2 \cdot n\text{CH}_2\text{Cl}_2$ (**2–4**) linked by a series of bridging ligands 4,4'-bipy, bpete and 4,4'-azpy have been synthesized. The crystal structure of **1** reveals a strongly distorted tetrahedral configuration, whereas **2–4** have a centrosymmetric diimine-bridging dinuclear structure with intrametallic distance being 11.194 Å, 12.436 Å and 13.130 Å, respectively. All of these complexes have relatively high thermal stability and exhibit low-energy absorption bands from 360 to 650 nm, corresponding to a MLCT transition. The binuclear complexes **2** and **3** both display a weak red emission from metal-to-ligand charge-transfer excited state. It is also noted that the EPR spectral data for complexes **1–4** all

reveal a formation of such copper(II)–halide complexes upon excitation at 355 nm in dichloromethane solution.

Acknowledgments

The work was supported by the State Key Project (No. 2005CCA06800), the National Natural Science Foundation of China (NSFC Grant Nos. 50463001 and 20671094) and Virtual Laboratory for Computational Chemistry, CNIC, CAS. We thank the foundation (50418010) for NSFC/RGC Joint Research.

Appendix A. Supplementary material

CCDC 615571, 615572, 615573 and 615574 contain the supplementary crystallographic data for **1**, **2**, **3** and **4**. These data can be obtained free of charge via <http://www.ccdc.cam.ac.uk/conts/retrieving.html>, or from the Cambridge Crystallographic Data Centre, 12 Union Road, Cambridge CB2 1EZ, UK; fax: (+44) 1223-336-033; or e-mail: deposit@ccdc.cam.ac.uk. Supplementary data associated with this article can be found, in the online version, at [doi:10.1016/j.ica.2007.02.007](https://doi.org/10.1016/j.ica.2007.02.007).

References

- [1] D.R. McMillin, K.M. McNett, *Chem. Rev.* 98 (1998) 1201.
- [2] V.W.W. Yam, K.K.W. Lo, *Chem. Soc. Rev.* 28 (1999) 323.
- [3] Z. Mao, H.Y. Chao, Z. Hui, C.M. Che, W.F. Fu, K.K. Cheung, N. Zhu, *Chem. Eur. J.* 9 (2003) 2885.
- [4] S. Hu, J.C. Chen, M.L. Tong, B. Wang, Y.X. Yan, S.R. Batten, *Angew. Chem., Int. Ed.* 44 (2005) 5471.
- [5] Y.C. Liu, C.I. Li, W.Y. Yeh, G.H. Lee, S.M. Peng, *Inorg. Chim. Acta* 359 (2006) 2361.
- [6] P.C. Ford, A. Vogler, *Acc. Chem. Res.* 26 (1993) 220.
- [7] J.D. Barrie, B. Dunn, G. Hollingsworth, J.I. Zink, *J. Phys. Chem.* 93 (1989) 3958.
- [8] Y. Rondelez, O. Sénèque, M.N. Rager, A.F. Duprat, O. Reinaud, *Chem. Eur. J.* 6 (2000) 4218.
- [9] C.M. Che, Z. Mao, V.M. Miskowski, M.C. Tse, C.K. Chan, K.K. Cheung, D.L. Phillips, K.H. Leung, *Angew. Chem., Int. Ed.* 39 (2000) 4084.
- [10] C.C. Chou, C.C. Su, H.L. Tsai, K.H. Lii, *Inorg. Chem.* 44 (2005) 628.
- [11] M.T. Miller, T.B. Karpishin, *Inorg. Chem.* 38 (1999) 5246.
- [12] C.T. Cunningham, J.J. Moore, K.L.H. Cunningham, P.E. Fanwick, D.R. McMillin, *Inorg. Chem.* 39 (2000) 3638.
- [13] A. Edel, P.A. Marnot, J.P. Sauvage, *Nouv. J. Chim.* 8 (1984) 495.
- [14] N. Alonso-Vante, V. Ern, P. Chartier, C.O. Dietrich-Buchecker, D.R. McMillin, P.A. Marnot, J.P. Sauvage, *Nouv. J. Chim.* 7 (1983) 3.
- [15] E.C. Riesgo, Y.Z. Hu, R.P. Thummel, *Inorg. Chem.* 42 (2003) 6648.
- [16] L. Gutiérrez, G. Alzuet, J. Borrás, A. Castiñeiras, A. Rodríguez-Forteza, E. Ruiz, *Inorg. Chem.* 40 (2001) 3089.
- [17] W.F. Fu, X. Gan, C.M. Che, Q.Y. Cao, Z.Y. Zhou, N.Y. Zhu, *Chem. Eur. J.* 10 (2004) 2228.
- [18] P.C. Ford, E. Cariati, J. Bourassa, *Chem. Rev.* 99 (1999) 3625.
- [19] P. Lugo-Ponce, D.R. McMillin, *Coord. Chem. Rev.* 208 (2000) 169.
- [20] M.T. Miller, P.K. Gantzel, T.B. Karpishin, *J. Am. Chem. Soc.* 121 (1999) 4292.
- [21] R.M. Williams, L. De Cola, F. Hartl, J.J. Lagref, J.M. Planeix, A. De Cian, M.W. Hosseini, *Coord. Chem. Rev.* 230 (2002) 253.
- [22] Q.Y. Cao, X. Gan, W.F. Fu, *Chin. J. Chem.* 22 (2004) 1283.

- [23] G.J. Kubas, B. Monzyk, A.L. Crumbliss, *Inorg. Synth.* 28 (1990) 68.
- [24] J.F. Norris, B.M. Sturgis, *J. Am. Chem. Soc.* 61 (1939) 1413.
- [25] C.E. Maxwell, *Org. Synth. Coll.* 3 (1955) 305.
- [26] F. Kröhnke, *Synthesis* (1976) 1.
- [27] J.P. Launay, T.P. Myriam, J.F. Lipskier, V. Marvaud, C. Joachim, *Inorg. Chem.* 30 (1991) 1033.
- [28] (a) G.M. Sheldrick, *SHELXS-97: Program for the Solution of Crystal Structures*, University of Göttingen, Göttingen, Germany, 1997;
(b) G.M. Sheldrick, *SHELXL-97: Program for the Solution of Crystal Structures*, University of Göttingen, Göttingen, Germany, 1997.
- [29] M.J. Frisch, G.W. Trucks, H.B. Schlegel, et al., *GAUSSIAN-03, Revision C.02*, Gaussian Inc., Wallingford, CT, 2004.
- [30] V. Kalsani, M. Schmittel, A. Listorti, G. Accorsi, N. Armaroli, *Inorg. Chem.* 45 (2006) 2061.
- [31] C. He, S.J. Lippard, *Inorg. Chem.* 39 (2000) 5225.
- [32] G. Kickelbick, U. Reinöhl, T.S. Ertel, A. Weber, H. Bertagnolli, K. Matyjaszewski, *Inorg. Chem.* 40 (2001) 6.
- [33] Z. Tyeklár, R.R. Jacobson, N. Wei, N.N. Murthy, J. Zubieta, K.D. Karlin, *J. Am. Chem. Soc.* 115 (1993) 2677.
- [34] T. Osako, K.D. Karlin, S. Itoh, *Inorg. Chem.* 44 (2005) 410.
- [35] J.M. Kern, J.P. Sauvage, *J. Chem. Soc., Chem. Commun.* (1987) 546.
- [36] L.F. Jia, W.F. Fu, Q. Yin, M.M. Yu, J.F. Zhang, Z.X. Li, *Acta Crystallogr., Sect. E* 61 (2005) 1039.